INTERNATIONAL JOURNAL OF PHARMACEUTICAL SCIENCES
[ISSN: 0975-4725; CODEN(USA): IJPS00]
Journal Homepage: https://www.ijpsjournal.com

OPEN ACCESS

Research Paper

Effect of Annealing Temperature on the Structural and Physicochemical Properties of Green-Synthesized Iron Oxide Nanoparticles from Ocimum sanctum

Shubhangi Pawar[1]*, Nilesh Pandit[2], Rajan More[3]

[1,3] Department of Zoology and Fisheries, Yashavantrao Chavan Institute of Science, Satara- 415 001 Maharashtra, India
[2]Department of Chemistry, Yashavantrao Chavan Institute of Science, Satara- 415 001 Maharashtra, India.

ARTICLE INFO

Published: 26 May 2026
Keywords:
Ocimum sanctum; green synthesis; iron oxide nanoparticles; annealing temperature; Crystallinity
DOI:
10.5281/zenodo.20392833

ABSTRACT

The present study investigates the effect of annealing temperature on the structural and physicochemical properties of iron oxide nanoparticles (Fe_2O_3 NPs) synthesized via an eco-friendly green route using Ocimum sanctum (Tulsi) leaf extract. Green synthesis provides a sustainable and cost-effective alternative to conventional chemical methods by eliminating the use of toxic reagents and high-energy processes. The phytochemicals present in O. sanctum, including eugenol, apigenin, rosmarinic acid, ursolic acid, flavonoids (orientin and vicenin), terpenoids, flavonols, and glucosides, act as natural reducing and stabilizing agents, facilitating efficient nanoparticle formation. The synthesized nanoparticles were annealed at 300, 500, and 700 °C to evaluate the influence of thermal treatment. UV–Visible spectroscopy confirmed nanoparticle formation, exhibiting characteristic absorption in the 200–300 nm region. The optical band gap, determined using Tauc plot analysis, decreased from 3.16 to 2.76 eV with increasing annealing temperature, indicating enhanced crystallinity and reduced quantum confinement. X-ray diffraction analysis confirmed the formation of phase-pure rhombohedral α-Fe_2O_3 with improved crystallinity at higher temperatures. Fourier transform infrared spectroscopy revealed Fe–O bond formation and progressive removal of phytochemical capping agents upon annealing. Scanning electron microscopy demonstrated morphological evolution from agglomerated particles at 300 °C to more uniform structures at 500 °C, followed by excessive grain growth at 700 °C. Energy-dispersive X-ray analysis confirmed improved elemental purity with increasing temperature. The sample annealed at 500 °C exhibited optimal structural and morphological properties. These findings demonstrate that controlled annealing is an

***Corresponding Author:** Shubhangi Pawar
Address: *Department of Zoology and Fisheries, Yashavantrao Chavan Institute of Science, Satara- 415 001 Maharashtra, India*
Email ✉: pawarshubhangi633@gmail.com

Relevant conflicts of interest/financial disclosures: The authors declare that the research was conducted in the absence of any commercial or financial relationships that could be construed as a potential conflict of interest.

effective strategy to tailor the properties of green-synthesized Fe_2O_3 nanoparticles for potential functional applications.

INTRODUCTION

Green synthesis represents an environmentally responsible and sustainable strategy for producing nanoparticles, offering a clear advantage over conventional techniques that typically rely on toxic reagents and substantial energy input [1]. Using plant extracts such as those derived from *Ocimum sanctum* provides a particularly effective route for the fabrication of iron oxide nanoparticles due to the plant's abundance of bioactive compounds [2]. This process minimizes environmental damage while simultaneously improving the biological compatibility and useful applications of the produced nanoparticles [3]. The thermal treatment applied during annealing plays a decisive role in modifying the structural and physicochemical characteristics of these nanoparticles, influencing parameters such as crystallinity, phase composition, and morphology [4]. As an eco-friendly methodology, green synthesis is increasingly valued in nanoparticle research for its ability to utilize naturally derived reducing and stabilizing agents in place of synthetic chemicals, thereby lowering production costs, minimizing hazardous waste, and reducing environmental impact [1].

In this context, *O. sanctum* leaf extract offers substantial benefits because it contains a diverse array of phytochemicals—including eugenol, flavonoids, tannins, alkaloids, terpenoids, and phenolic compounds that effectively facilitate reduction and stabilization processes during nanoparticle formation [2, 5, 6]. These naturally occurring metabolites enable the synthesis of iron oxide nanoparticles with enhanced purity, better crystallinity, and more controlled particle dimensions, ultimately improving their structural integrity and physicochemical performance [2]. Annealing plays an important role in determining the structural evolution of nanoparticles, exerting a strong influence on their crystallinity and phase behaviour [4]. In the case of iron oxide nanoparticles, thermal treatment promotes the growth of well-defined crystalline structures, drives phase transitions, and helps reduce lattice imperfections. This process is particularly important for inducing the transformation of maghemite (γ-Fe_2O_3) into the more thermodynamically stable hematite (α-Fe_2O_3), thereby enhancing structural order and altering magnetic characteristics [4]. Such modifications are essential for fine-tuning the properties of iron oxide nanoparticles to meet the requirements of targeted technological and biomedical applications [7, 8]. Previous research has demonstrated that plant-mediated synthesis of Fe_2O_3 nanoparticles provides an eco-friendly and sustainable alternative to traditional chemical methods [9].

Plant extracts enriched with phytochemicals such as flavonoids, polyphenols, and other bioactive compounds act simultaneously as reducing and stabilizing agents, thereby influencing nanoparticle dimensions, morphology, and overall stability [10]. Numerous studies have successfully produced Fe_2O_3 nanoparticles with enhanced catalytic and biological activities using plant sources, including *Citrus limetta*, *Hibiscus*, and *Phyllanthus niruri* [11, 9, 12]. Annealing temperature plays a decisive role in further modifying these green-synthesized nanoparticles, as thermal treatment strongly affects their crystalline structure, particle size, and phase composition [4, 7, 13, 14]. Typically, increasing the annealing temperature improves crystallinity and increases crystallite size, reflecting the reorganization and growth of crystalline domains. This heating process also drives phase transformations, particularly the conversion of magnetite or maghemite (γ-Fe_2O_3) into the more

stable hematite (α-Fe_2O_3), which subsequently alters their optical absorption and magnetic response [15, 7, 13]. Additionally, higher annealing temperatures help refine nanoparticle morphology by promoting uniformity and reducing structural defects [4, 7]. Studies consistently show that heating at 500–900 °C facilitates the transition from γ-Fe_2O_3 to α-Fe_2O_3, ultimately yielding nanoparticles with superior crystallinity and improved magnetic properties [7].

A clear research gap exists in the current literature regarding the relationship between *Ocimum sanctum*–mediated green synthesis of iron oxide nanoparticles and the role of post-synthesis thermal treatment. Although many studies have explored the biosynthesis of iron oxide nanoparticles using *O. sanctum* and the independent effects of annealing on nanoparticle behaviour, comprehensive investigations linking these two aspects remain limited. Most available reports emphasize synthesis and preliminary characterization but lack detailed evaluations of how different annealing temperatures modify the structural, morphological, and physicochemical features of nanoparticles produced through this plant extract. In particular, systematic studies are needed to understand how controlled thermal treatment influences critical transitions—such as the transformation from maghemite (γ-Fe_2O_3) to hematite (α-Fe_2O_3)—and other key material properties when *O. sanctum* is employed as the reducing and stabilizing agent.

This study aims to provide a systematic assessment of how varying annealing temperatures influence the structural, morphological, optical, magnetic, and overall physicochemical characteristics of iron oxide nanoparticles synthesized through a green route. It specifically addresses the existing gap in the literature by delivering a detailed examination of the relationship between thermal treatment conditions and the resulting properties of Fe_2O_3 nanoparticles produced using *Ocimum sanctum* leaf extract. The objective is to clarify how controlled annealing drives structural transformations and property modifications in these nanoparticles, ultimately generating valuable insights for precisely tailoring their features to meet the requirements of targeted technological and biological applications.

2. MATERIALS AND METHODS

2.1 Plant Material Collection:

Fresh and healthy leaves of *Ocimum sanctum* (commonly known as Krishna tulsi) were collected from the botanical garden of Yashwantrao Chavan Institute of Science, Satara, and were identified by the Department of Botany. Further authentication with the help of the herbarium. The leaves were thoroughly washed several times with tap water, followed by distilled water to remove dust and surface contaminants. The cleaned leaves were shade-dried at room temperature until completely moisture-free.

2.2 Reagents and chemicals:

The chemicals used in this study were of analytical grade and used without further purification. Ferrous sulfate heptahydrate ($FeSO_4 \cdot 7H_2O$), NaOH, and H_2SO_4 for pH adjustment were purchased from Bio Treasure India Scientific Centre. Double-distilled water was used throughout the synthesis process.

2.3 *Ocimum sanctum* leaf extract preparation:

The aqueous extract of *Ocimum sanctum* leaves was prepared using the hot infusion method to extract bioactive phytochemicals responsible for the reduction and stabilization of iron oxide nanoparticles. Fresh green leaves of *Ocimum sanctum* (approx. 20 grams) were thoroughly washed with tap water, followed by distilled water to remove dust and surface impurities. The cleaned leaves were then chopped into small pieces and boiled in 100 mL of distilled water at 70–80°C for

15–20 minutes. During heating, the mixture was gently stirred to ensure maximum extraction of active compounds into the solution. After boiling, the extract was allowed to cool to room temperature. It was then filtered using Whatman No. 1 filter paper to remove leaf residues and obtain a clear filtrate. The resulting light brown to greenish extract was collected in a sterile container and stored at 4°C. The extract was used within 24-48 hours to ensure the stability of the phytochemicals during the nanoparticle synthesis process.

2.4 Green Synthesis of Iron Oxide Nanoparticles:

The green synthesis of iron oxide (Fe_2O_3) nanoparticles was carried out using the aqueous leaf extract of *Ocimum sanctum* as both a reducing and stabilizing agent. This eco-friendly method eliminates the need for hazardous chemicals typically used in conventional synthesis. A 0.1 M solution of ferrous sulfate heptahydrate ($FeSO_4 \cdot 7H_2O$) was prepared by dissolving the appropriate amount in double-distilled water, adding H_2SO_4 dropwise to prevent oxidation of Fe ions. Iron oxide nanoparticles were synthesized by mixing 100 mL of 0.1 M ($FeSO_4 \cdot 7H_2O$) with a 50 mL solution of freshly prepared *Ocimum sanctum* leaf extract, which was added in a 1:2 volume ratio under constant stirring at room temperature. The pH of the solution was kept at 8 using .0 M NaOH solution reaction mixture, which was maintained stirred at 60–70°C for 50-60 minutes to facilitate the reduction of Fe^{2+} ions and the formation of iron oxide nanoparticles, and NaOH (1.0 M stock) was added for pH adjustment. The gradual colour change from yellowish-brown to dark brown (black) indicated the formation of iron oxide nanoparticles. The reaction mixture was allowed to cool, and the precipitate was collected by centrifugation at 7500 rpm for 15 minutes. The pellet was washed several times with distilled water and ethanol to remove any unbound phytochemicals or impurities, and dried at 80 °C for 12 h. The dried powder was stored for subsequent annealing.

2.5 Annealing of synthesized nanoparticles:

After drying, the green-synthesized iron oxide (Fe_2O_3) nanoparticles were subjected to controlled annealing to investigate the effect of thermal treatment on their structural and morphological properties. Approximately 500 mg of dried Iron oxide nanoparticles were placed into high-purity ceramic crucibles and annealed in a programmable muffle furnace at four different temperatures: 300°C, 500°C, and 700°C for 3 hours each. The primary purpose of annealing was to improve crystallinity, remove residual organic compounds (such as plant metabolites), and promote phase transformation. After annealing, the furnace was allowed to cool gradually to room temperature. The samples were labeled according to their annealing temperature and stored in airtight containers for further characterization.

2.6 Characterization of nanoparticles.

The green-synthesized iron oxide nanoparticles (IONPs) annealed at different temperatures were characterized by using UV-visible spectroscopy, X-ray Diffraction (XRD), Fourier transform infrared spectroscopy (FTIR), and scanning electron microscopy (SEM-EDX) to evaluate their structural, morphological, optical, and elemental properties

3. RESULTS AND DISCUSSION

3.1 UV-Visible Spectroscopy Analysis:

The UV–Visible absorption spectra of green-synthesized iron oxide nanoparticles (Fe_2O_3 NPs) using *Ocimum sanctum* leaf extract, along with samples annealed at 300°C, 500°C, and 700°C, are presented in Fig. 1. All samples exhibit strong absorption in the ultraviolet region (200–300 nm),

which is characteristic of iron oxide nanoparticles and is attributed to ligand-to-metal charge transfer transitions between O^{2-} and Fe^{3+} ions. The unannealed sample (O.S) shows the highest absorbance intensity (~0.75 at 200 nm), which can be attributed to the presence of phytochemicals such as flavonoids, phenolics, and proteins from *Ocimum sanctum* acting as capping and stabilizing agents. These biomolecules contribute to enhanced optical density and broader absorption features. With increasing annealing temperature, absorbance intensity gradually decreases, particularly in the visible region (400–800 nm). This reduction indicates the thermal decomposition of organic capping agents and the removal of residual impurities, leading to improved purity and structural ordering of the nanoparticles. The absorption curves also become smoother with increasing temperature, suggesting reduced surface defects and enhanced crystallinity. A slight shoulder observed in the 250–300 nm region is associated with surface interactions and residual phytochemicals, which diminish upon annealing. Overall, the UV–Vis analysis confirms the successful synthesis of iron oxide nanoparticles. These observations confirm that annealing significantly influences the optical behaviour of Fe_2O_3 nanoparticles.

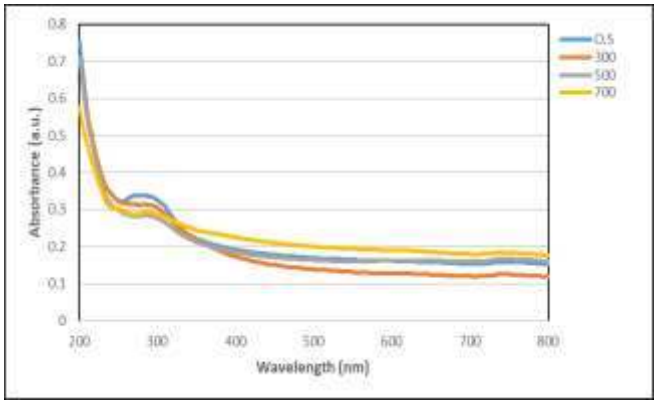

Fig. 1. UV–Visible absorption spectra of green-synthesized iron oxide nanoparticles prepared using *Ocimum sanctum* leaf extract at different annealing temperatures. (O.S – *Ocimum sanctum* extract, 300 °C, 500 °C, 700 °C)

Tauc Plot of Green-Synthesized Fe_2O_3 Nanoparticles Derived from *Ocimum sanctum* and Annealed at Different Temperatures

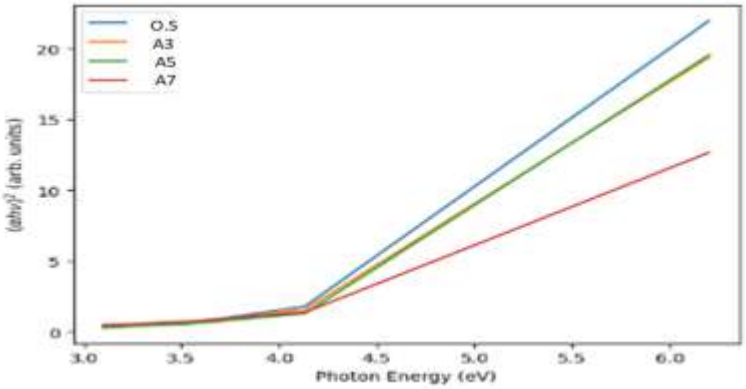

Fig. 2. Tauc plots $(\alpha h\nu)^2$ versus photon energy $(h\nu)$ for Fe_2O_3 nanoparticles synthesized using *Ocimum sanctum* leaf extract and annealed at different temperatures (300°C, 500°C, and 700°C).

The optical band gap of Fe_2O_3 nanoparticles was determined using the Tauc plot shown in Figure 2 $(\alpha h\nu)^2$vs. $h\nu$, showing a decrease from 3.16 eV (O.S) to 3.06 eV (300°C), 2.96 eV (500°C), and 2.76 eV (700°C). This reduction with increasing annealing temperature is attributed to crystallite growth, reduced quantum confinement, improved crystallinity, and the formation of defect states such as oxygen vacancies. The higher band gap values compared to bulk α-Fe_2O_3 (~2.1 eV) confirm the nanoscale nature of the samples, while the decreasing trend indicates a shift toward bulk-like behaviour. The results agree with reported literature (2.2–3.1 eV range). The estimated error (±0.02–0.05 eV) mainly arises from linear region selection in the Tauc plot, instrumental limitations, and the use of absorbance instead of absorption coefficient, with minor effects from scattering and baseline correction.

XRD:

The X-ray diffraction (XRD) patterns of green-synthesized iron oxide nanoparticles annealed at 300,500 and 700 °C (Figure 3; Table 1) reveal a clear temperature- dependent evolution in phase composition, crystallinity, and crystallite size, consistent with the standard JCPDS card No. 00-033-0664 corresponding to rhombohedral α-Fe_2O_3 (hematite). At 300 °C, the diffraction pattern exhibits broad and low-intensity peaks at 2θ ≈ 18.2° (100), 23.5° (110), and 29.8° (200), which are associated with iron oxalate hydrate and intermediate phases, indicating incomplete crystallization. Weak reflections observed at ~35.6° (211), 43.2° (220), and 57.1° (311) suggest the initial formation of the Fe_3O_4 phase. The broadness of these peaks reflects poor crystallinity and smaller crystallite size due to structural disorder, which is consistent with previous reports on low- temperature green-synthesized iron oxide nanoparticles [16] [17]. At 500 °C, the diffraction peaks become sharper and more intense, indicating improved crystallinity and phase development. Prominent peaks at 2θ ≈ 30.1° (220), 35.5° (311), 43.1° (400), 53.5° (422), 57.0° (511), and 62.6° (440) correspond to the characteristic planes of cubic spinel Fe_3O_4, confirming the formation of a well-defined magnetite phase. The reduced peak broadening and increased intensity indicate enhanced crystallite growth and better structural ordering. Such improvements in crystallinity with increasing annealing temperature have been widely reported in green synthesis studies, where thermal treatments facilitate decomposition of organic residues and promote stabilization [9]. Upon further annealing at 700 °C, a complete phase to α-Fe_2O_3 (hematite) is observed, as evidenced by the appearance of strong and sharp diffraction peaks at 2θ ≈ 24.1° (012), 33.2° (104), 35.6° (110), 40.9° (113), 49.5° (024), 54.1° (116), 57.6° (018), and 62.5° (214), which are in excellent agreement with JCPDS card NO. . 00-033-0664. The high intensity and sharpness of these peaks confirm the formation of a highly crystalline and phase-pure hematite structure. However, the significant narrowing of peaks at this temperature indicates excessive grain growth and particle agglomeration. Which is also consistent with recent findings, where higher annealing temperature leads to increased crystallite size (~40–70 nm) due to thermal coalescence [18]. Overall, the crystallite size increases progressively with annealing temperature, confirming thermally induced grain growth and reduction in lattice strain. While the 700 °C sample exhibits crystallinity, the associated increase in particle size may limit surface-dependent properties such as antibacterial activity. In contrast, the 500 °C sample offers an optimal balance between crystallinity, phase purity, and nanoscale crystallite size, making it more suitable for applications requiring high surface reactivity. This trend is in strong agreement with recent literature, where moderate annealing temperatures are

reported to yield nanoparticles with superior functional performance due to their favourable size and properties [16] [9]

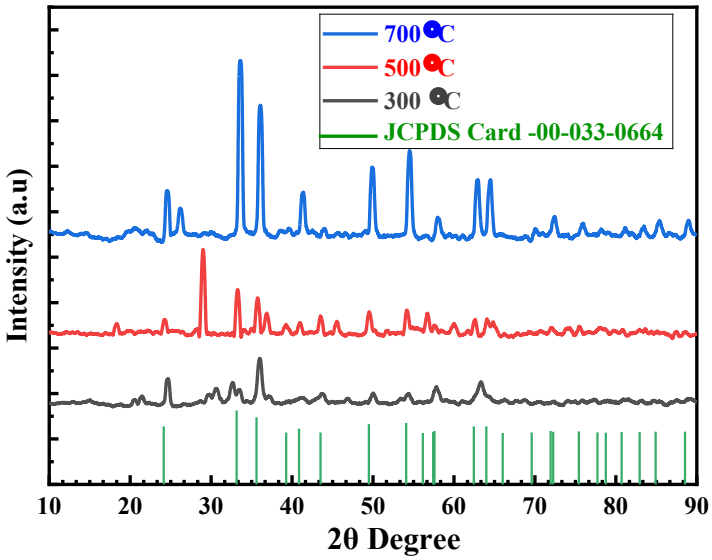

Fig. 3. X-ray diffraction patterns of iron oxide nanoparticles synthesized using *Ocimum sanctum* leaf extract and annealed at 300, 500, and 700 °C, compared with the standard JCPDS card No. 00-033-0664 of α-Fe_2O_3 (hematite), showing enhanced crystallinity and phase stabilization with increasing annealing temperature.

Table 1: XRD peak positions, phase identification, and crystallite size of iron oxide nanoparticles at different annealing temperatures

Temperature (°C)	2θ (°)	D-Spacing (Å)	Relative Intensity	Plane (hkl)	Phase	Crystallite Size (nm)
300	18.2	4.87	Low	(100)	Iron oxalate hydrate	~15
	23.5	3.78	Medium	(110)	Intermediate	~16
	29.8	2.99	Medium	(200)	Intermediate	~17
	35.6	2.52	Weak	(211)	Fe_3O_4 (initial)	~18
	43.2	2.09	Weak	(220)	Fe_3O_4	~20
	57.1	1.61	Weak	(311)	Fe_3O_4	~22
500	30.1	2.96	Strong	(220)	Fe_3O_4	~28
	35.5	2.52	Very Strong	(311)	Fe_3O_4	~32
	43.1	2.09	Medium	(400)	Fe_3O_4	~30
	53.5	1.71	Medium	(422)	Fe_3O_4	~33
	57.0	1.61	Strong	(511)	Fe_3O_4	~35
	62.6	1.48	Medium	(440)	Fe_3O_4	~34
700	24.1	3.69	Medium	(012)	Fe_2O_3 (Hematite)	~42
	33.2	2.69	Very Strong	(104)	Fe_2O_3	~45
	35.6	2.52	Strong	(110)	Fe_2O_3	~48
	40.9	2.20	Medium	(113)	Fe_2O_3	~47
	49.5	1.84	Medium	(024)	Fe_2O_3	~50

	54.1	1.69	Medium	(116)	Fe_2O_3	~49
	57.6	1.60	Strong	(018)	Fe_2O_3	~51
	62.5	1.48	Strong	(214)	Fe_2O_3	~52

FTIR:

The FTIR spectra of green-synthesized iron oxide nanoparticles annealed at 300, 500, and 700 °C are presented in Figure 4, and Table No. 2 to evaluate the influence of annealing temperature on surface functionalization and Fe–O bond formation. All samples exhibit characteristic absorption bands in the low-wavenumber region below 700 cm^{-1}, corresponding to Fe–O stretching vibrations, confirming the successful formation of iron oxide nanoparticles. The nanoparticle sample annealed at 500 °C exhibits well-defined Fe–O vibrational bands along with noticeable absorption features in the 1000–1600 cm^{-1} region, attributed to residual phytochemical functional groups such as C–O, C=O, and O–H vibrations derived from *Ocimum sanctum* leaf extract. The presence of these functional groups indicates that the nanoparticles retain a suitable amount of bioactive organic capping even after annealing, which may enhance surface stability, dispersibility, and biological interaction.

Upon increasing the annealing temperature to 500 and 700 °C, the intensity of these phytochemical-associated bands progressively decreases, indicating thermal decomposition and removal of the organic capping agents. Although higher annealing temperatures improve phase purity and crystallinity, excessive thermal treatment leads to a significant loss of surface-bound phytochemicals and may promote particle agglomeration due to the absence of stabilizing organic moieties. Therefore, the sample annealed at 500 °C appears to provide the most favourable balance between successful iron oxide formation and retention of phytochemical surface functionality, making it the optimal annealing temperature for preserving both structural integrity and biologically relevant surface chemistry. This retained organic functionality may contribute positively to enhanced antibacterial and surface-reactive properties of the nanoparticles.

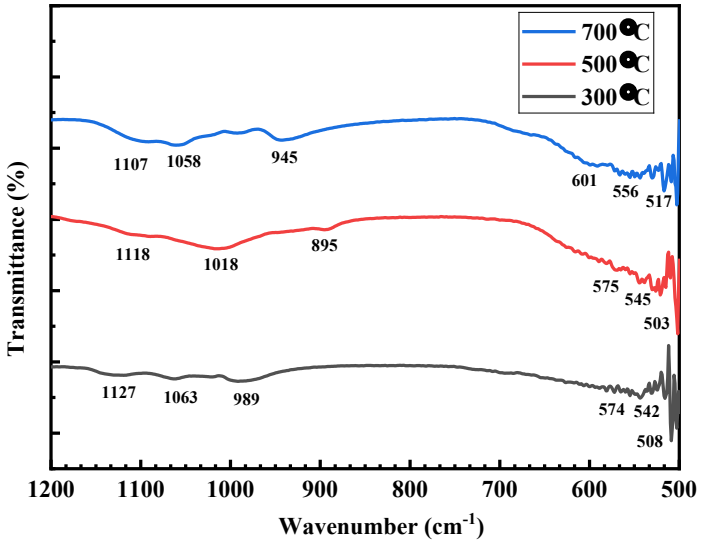

Fig. 4. FTIR spectra of green-synthesized iron oxide nanoparticles derived from *Ocimum sanctum* leaf extract annealed at 300, 500, and 700 °C, showing the progressive removal of phytochemical residues and the strengthening of characteristic Fe–O stretching vibrations with increasing annealing temperature.

Table 2. Comparative FTIR Peak Assignment Table with Temperature Effect

Wavenumber (cm^{-1})	300 °C (Black)	500 °C (Red)	700 °C (Blue)	Assignment	Thermal Interpretation
3400–3200	Weak	Moderate	Weak / very weak	O–H stretching	Loss of moisture and hydroxyl groups with increasing temperature
2920–2850	Weak	Moderate	Very weak	C–H stretching	Decomposition of aliphatic chains at higher temperatures
1740–1700	Weak	Moderate	Absent	C=O stretching	Carbonyl groups form at mid-temp, then decompose at high temp
1650–1600	Weak	Moderate	Weak	C=C / Amide I	Aromatic structures begin forming, then stabilize
1540–1500	Weak	Moderate	Weak	Amide II	Protein structures degrade with heating
1450–1400	Weak	Moderate	Weak	CH_2 bending	Gradual loss of organic components
1370–1300	Weak	Moderate	Weak	C–H bending	Decreasing aliphatic content
1250–1200	Weak	Moderate	Weak	C–O stretching	Breakdown of esters/polysaccharides
1150–1000	Moderate	Strong	Moderate–weak	C–O–C / C–O	Carbohydrates degrade, peak strongest at 500 °C
900–700	Weak	Weak	Weak–moderate	Aromatic C–H	Formation of aromatic/graphitic structures
<700	Noisy	Noisy	Strong noisy peaks	Fingerprint region	Increased structural disorder/mineral residues

3.4 Scanning Electron Microscopy (SEM)

1) SEM Analysis of Iron Oxide Nanoparticles Annealed at 300 °C

The surface morphology of the iron oxide nanoparticles annealed at 300 °C was examined by scanning electron microscopy (SEM), and the corresponding micrographs are shown in Figure 5(a–d). The SEM images reveal that the nanoparticles possess an irregular and highly agglomerated morphology, forming clustered aggregates with rough and non-uniform surfaces. Such agglomeration is commonly observed in green-synthesized iron oxide nanoparticles due to the particle's magnetic nature and the presence of residual phytochemical capping agents from *Ocimum sanctum* extract.

At lower magnification, the nanoparticles appear as densely packed aggregates distributed over the surface, while higher magnification images indicate that the agglomerates are composed of interconnected nanosized particles with indistinct boundaries. The incomplete particle separation suggests that annealing at 300 °C is insufficient for full removal of the organic phytochemical coating

and for achieving well-defined crystalline particle growth. This observation is consistent with the XRD and FTIR results, which indicate lower crystallinity and the retention of plant-derived functional groups at lower annealing temperatures. Particle size measurements from selected SEM micrographs indicate that the agglomerated nanoparticle domains possess an average size in the range of approximately 53–58 nm, confirming nanoscale dimensions despite aggregation. The irregular morphology and relatively smaller particle size at 300 °C suggest incomplete grain growth and partial structural ordering during low-temperature annealing. Overall, the 300 °C annealed sample exhibits nanosized but poorly defined and highly aggregated iron oxide particles with limited crystallinity.

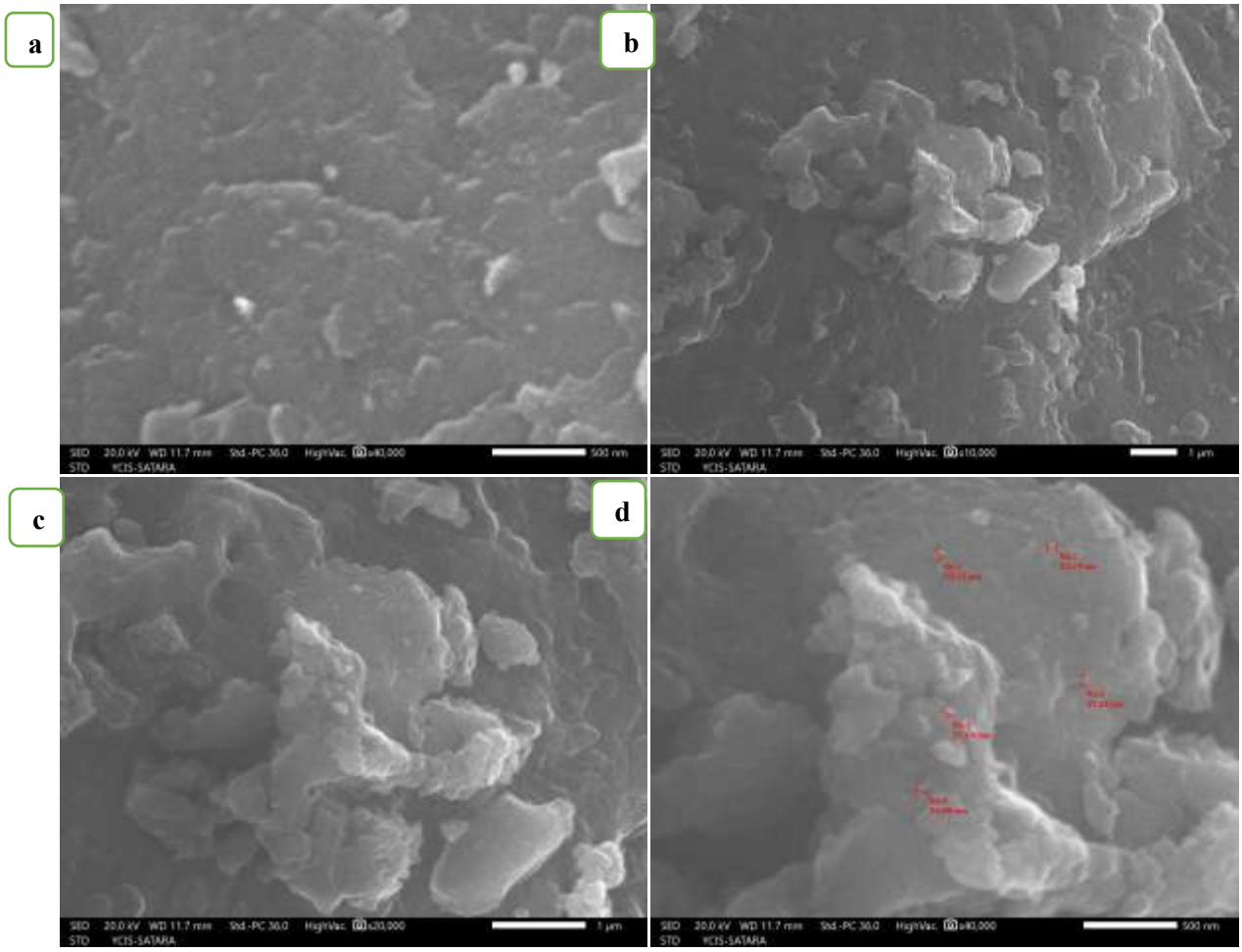

Fig. 5 (a–d) SEM micrographs of green-synthesized iron oxide nanoparticles annealed at 300 °C at different magnifications, showing irregular agglomerated morphology with nanoscale particle domains of approximately 53–58 nm.

2) SEM Analysis of Iron Oxide Nanoparticles Annealed at 500 °C

The SEM micrographs of iron oxide nanoparticles annealed at 500 °C are presented in Figure 5(e–h). Compared with the sample annealed at 300 °C, the 500 °C-treated sample exhibits a more homogeneous and well-defined granular morphology with improved particle separation and surface uniformity. The particles appear as nearly spherical to irregular nanograins aggregated into clustered domains, indicating enhanced structural development upon thermal treatment. The increased annealing temperature facilitates decomposition of residual phytochemical capping

agents and promotes improved crystallization, resulting in more distinguishable particle boundaries and reduced amorphous character. Although agglomeration is still evident—likely due to magnetic interactions and partial sintering of adjacent particles—the aggregates are more uniformly distributed compared with the 300 °C sample. The average particle/agglomerate size of the 500 °C annealed sample was determined to be approximately 264 nm**.** The relatively larger observed particle size compared to XRD-derived crystallite size suggests that the particles exist as aggregated secondary clusters composed of multiple smaller crystalline domains, which is commonly observed in iron oxide nanomaterials synthesized via green routes. Overall, the SEM results indicate that annealing at 500 °C yields particles with improved morphological uniformity and controlled agglomeration, suggesting that this temperature provides an optimal balance between enhanced crystallinity and preservation of favourable surface morphology for functional applications.

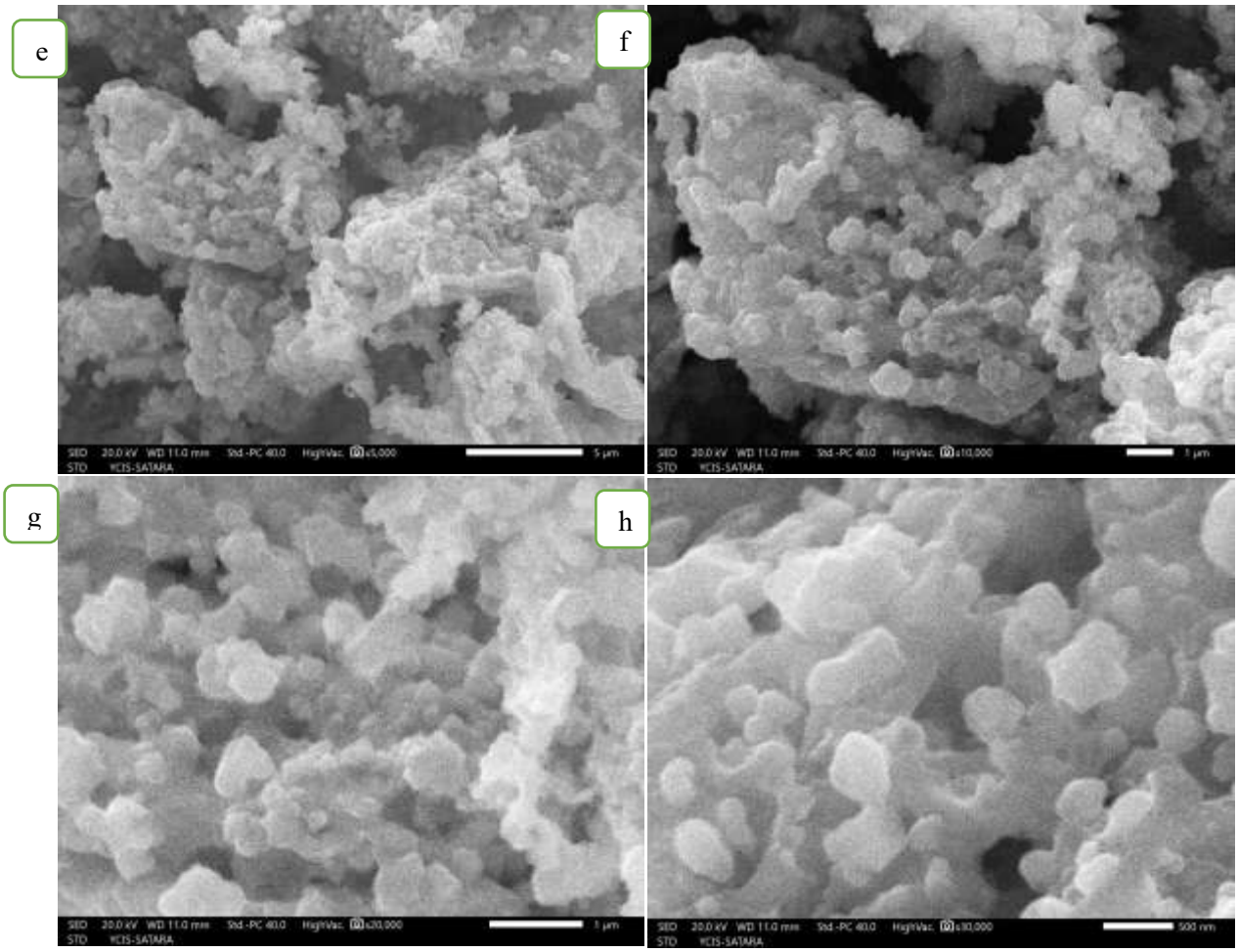

Fig. 5(e–h). SEM micrographs of green-synthesized iron oxide nanoparticles annealed at 500 °C, showing homogeneous granular morphology with particle sizes in the range of approximately 264 nm.

3) SEM Analysis of Iron Oxide Nanoparticles Annealed at 700 °C

The SEM micrographs of iron oxide nanoparticles annealed at 700 °C are shown in Figure 5(i–l). A significant change in morphology is observed compared with the samples annealed at lower temperatures. The 700 °C-treated sample exhibits highly fused, densely packed, and plate-like aggregated structures, indicating extensive grain growth and thermal sintering at elevated

temperature. The individual nanoparticle boundaries become less distinguishable, and the particles appear merged into larger compact domains due to coalescence during high-temperature annealing. The pronounced morphological transformation suggests that excessive thermal treatment promotes particle fusion, crystallite coarsening, and structural densification, resulting in a loss of discrete nanoscale particle morphology. The average particle/agglomerate size of the 700 °C annealed sample was found to be approximately 278 nm, which is higher than that observed for the 500 °C sample, confirming progressive particle growth and aggregation with increasing annealing temperature. Compared with the 500 °C annealed sample, which exhibited more uniformly distributed granular particles with smaller aggregate size, the 700 °C sample shows severe agglomeration and overgrowth of particle domains, which may reduce effective surface area and limit accessibility of active surface sites. Such excessive sintering can negatively affect surface-dependent properties including catalytic and antibacterial performance despite improved crystallinity. Overall, the SEM analysis confirms that annealing at 700 °C leads to excessive particle coalescence and morphological deterioration, suggesting that further increase in annealing temperature beyond 500 °C is detrimental to maintaining favourable nanoscale morphology of the iron oxide nanoparticles.

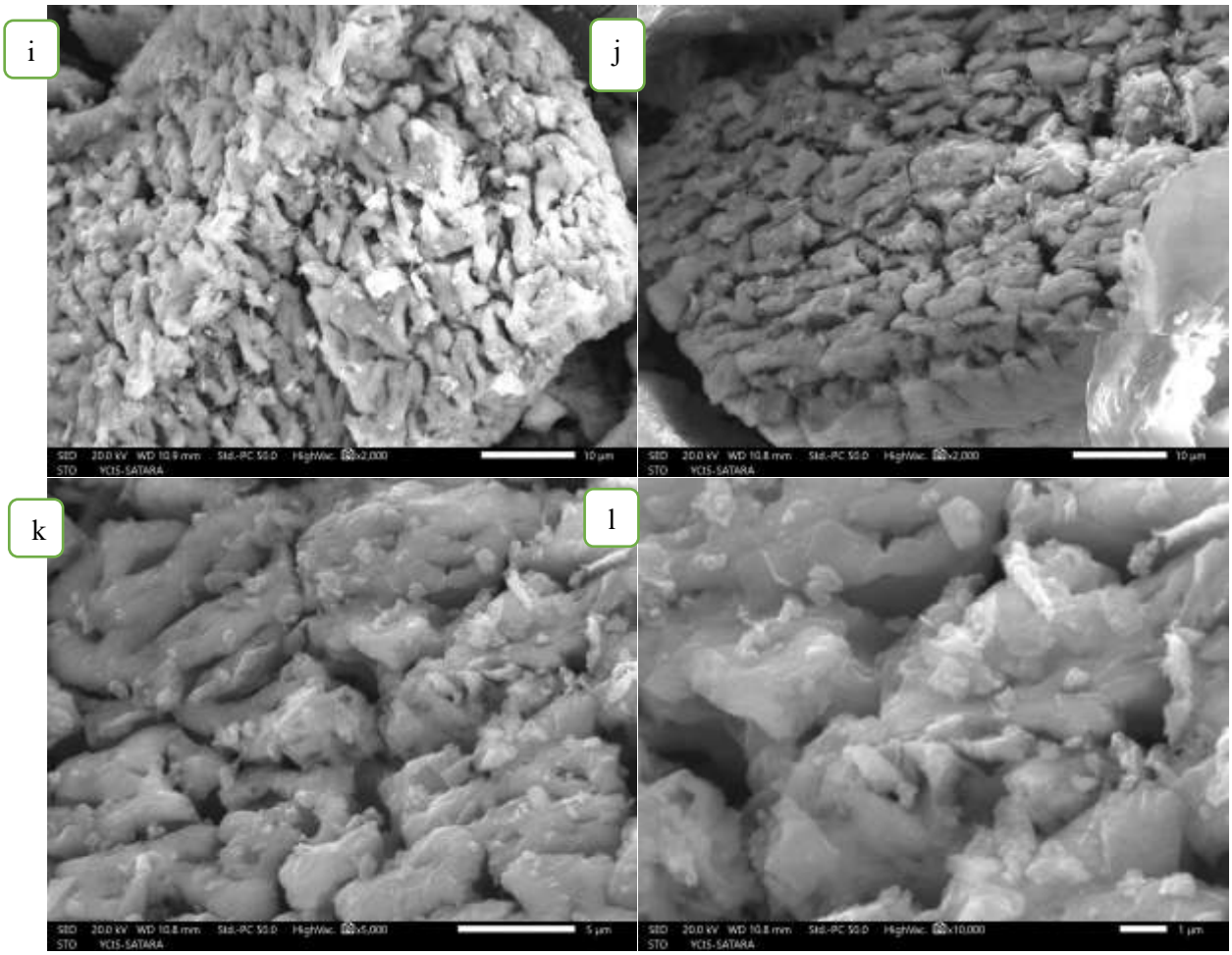

Fig. 5 (i–l). SEM micrographs of green-synthesized iron oxide nanoparticles annealed at 700 °C, showing fused plate-like aggregated morphology with an average particle/agglomerate size of approximately 278 nm, indicating significant thermal sintering and particle coalescence.

Comparative SEM Analysis

The morphological evolution of green-synthesized iron oxide nanoparticles with increasing annealing temperature was investigated by SEMs, as shown in Table No. 2, and the corresponding micrographs are presented in Figure 5(a–l). The sample annealed at 300 °C exhibits irregular and highly agglomerated particle clusters with poorly defined boundaries and rough surface morphology, indicating incomplete crystallization and the presence of residual phytochemical capping agents from *Ocimum sanctum* extract. The agglomerated domains at this temperature possess sizes in the range of approximately 53–58 nm, suggesting the formation of small but poorly ordered nanoscale particles. Upon annealing at 500 °C, the morphology becomes significantly more homogeneous and granular, with improved particle definition, enhanced surface uniformity, and reduced amorphous character. The particles appear as well-developed aggregated nanograins with an average particle/agglomerate size of approximately 264 nm, indicating enhanced structural ordering while preserving favourable nanoscale morphology. This suggests that annealing at 500 °C provides sufficient thermal energy to improve crystallinity and particle formation without causing excessive grain coalescence. In contrast, the sample annealed at 700 °C displays highly fused, densely packed, and plate-like aggregated structures with an increased average particle/agglomerate size of approximately 278 nm, reflecting substantial grain growth, particle coalescence, and thermal sintering at elevated temperature. The loss of discrete particle boundaries and formation of compact fused domains at 700 °C indicate morphological deterioration due to over-annealing. Overall, the comparative SEM analysis demonstrates that 500 °C is the optimal annealing temperature, providing the best balance between improved crystallinity, morphological uniformity, and controlled particle growth, whereas lower temperatures result in incomplete structural development and higher temperatures lead to excessive agglomeration and sintering.

Table 3: Morphological Characteristics of Fe_2O_3 Nanoparticles at Different Annealing Temperatures

Temperature	Phase	Chemical Formula	Crystal Structure	Morphological Characteristics	Particle Size	Key Observation
300°C	Iron Oxalate Hydrate	$FeC_2O_4 \cdot 2H_2O$	Semi-crystalline / precursor phase	Irregular, highly agglomerated clusters with rough, non-uniform surfaces; poorly defined particle boundaries	**53–58 nm**	Incomplete decomposition; presence of phytochemical residues; poor crystallinity
500°C	Magnetite (Intermediate phase)	Fe_3O_4	Cubic (mixed Fe^{2+}/Fe^{3+})	More homogeneous and granular morphology; nearly spherical to irregular nanograins forming clustered domains with improved particle separation	**~264 nm**	Enhanced crystallinity; controlled particle growth; optimal morphology

700°C	Hematite (Final phase)	Fe_2O_3 (α-phase)	Rhomboh edral	Highly fused, dense, plate-like aggregated structures due to thermal sintering; loss of discrete nanoparticle boundaries	**~278 nm**	Complete oxidation; excessive grain growth; particle coalescence, and reduced surface area

3.5 Energy-Dispersive X-ray Spectroscopy (EDX)

1) 300 EDX

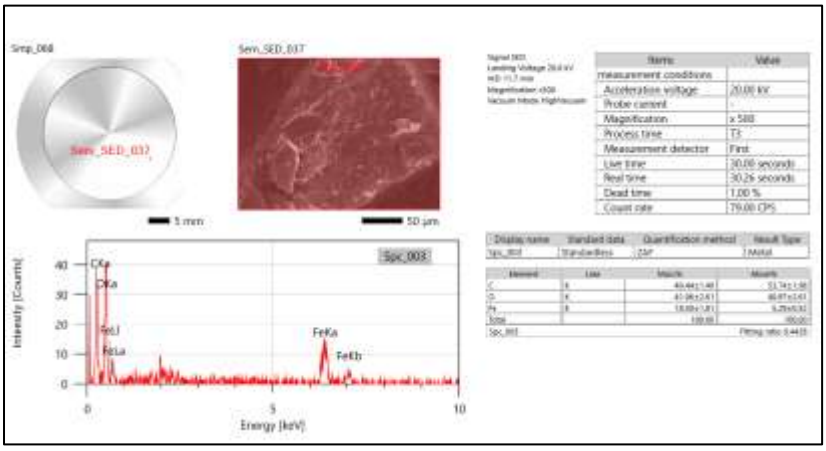

Fig. 6. Energy-Dispersive X-ray Spectroscopy (EDX) spectrum of the sample treated at 300 °C, illustrating its elemental composition and purity.

2) 500 EDX

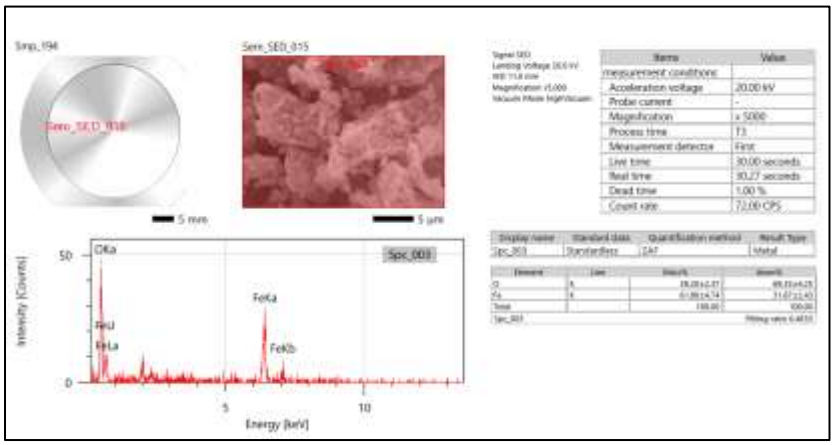

Fig. 7. Energy-Dispersive X-ray Spectroscopy (EDX) spectrum of the sample treated at 500 °C, illustrating its elemental composition and purity.

3) 700 EDX

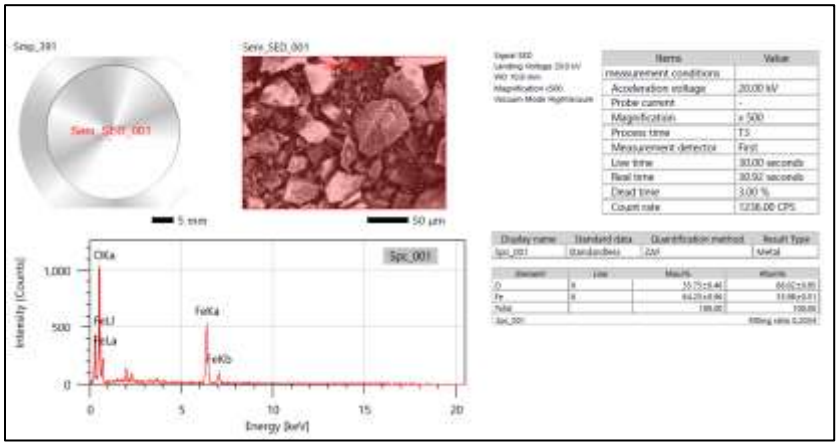

Fig. 8. Energy-Dispersive X-ray Spectroscopy (EDX) spectrum of the sample treated at 700 °C, illustrating its elemental composition and purity.

The elemental composition of the green-synthesized iron oxide nanoparticles annealed at 300, 500, and 700 °C was analysed by energy-dispersive X-ray spectroscopy (EDX), and the corresponding spectra are shown in Figures 6, 7, and 8. All samples exhibit prominent characteristic peaks corresponding to Fe and O, confirming the successful formation of iron oxide nanoparticles. The sample annealed at 300 °C shows the presence of C, O, and Fe, with carbon accounting for approximately 40.44 wt%, indicating the retention of significant residual organic phytochemical content from the *Ocimum sanctum* leaf extract due to incomplete thermal decomposition at a lower annealing temperature. Upon annealing at 500 °C, the carbon peak disappears completely, and only Fe and O signals are observed, with Fe and O contents of approximately 61.80 wt% and 38.20 wt%, respectively, confirming effective removal of organic residues and formation of relatively pure iron oxide nanoparticles. Further annealing at 700 °C results in an increase in Fe content to approximately 64.25 wt% with corresponding oxygen content of 35.75 wt%, indicating improved phase purity and densification of the oxide structure due to enhanced thermal crystallization. The gradual elimination of carbon impurities and increase in Fe content with rising annealing temperature demonstrate that thermal treatment significantly improves the compositional purity of the synthesized nanoparticles. Overall, the EDX results corroborate the FTIR, XRD, and SEM analyses, confirming progressive purification and structural refinement of iron oxide nanoparticles with increasing annealing temperature.

CONCLUSION

The present study successfully demonstrates the green synthesis of iron oxide (Fe_2O_3) nanoparticles using *Ocimum sanctum* leaf extract and highlights the significant influence of annealing temperature on their physicochemical properties. UV- Visible analysis confirmed nanoparticle formation, showing strong absorption in the UV region and a systematic decrease in optical band gap from 3.16 eV to 2.76 eV with increasing annealing temperature, indicating enhanced crystallinity, reduced quantum confinement, and particle growth. XRD results confirmed the formation of phase-pure rhombohedral α-Fe_2O_3 with improved crystallinity at higher temperatures, while FTIR analysis revealed the presence of Fe–O bonds and phytochemical functional groups that progressively diminished upon annealing due to thermal decomposition. SEM studies showed a clear morphological transformation from highly agglomerated and poorly defined nanoparticles at 300 °C to more uniform granular structures at 500 °C, followed by excessive particles fusion and

coalescence at 700 °C. EDX analysis confirmed the elemental composition and demonstrated a gradual reduction in carbon impurities as temperature increased, indicating improved compositional purity. Among the studied conditions, 500 °C was identified as the optimal annealing temperature, providing the best balance between crystallinity, nanoscale morphology, and retention of surface functional groups, which are crucial for surface-dependent application. Overall, this study established that controlled annealing of green-synthesized Fe_2O_3 nanoparticles is an effective strategy for tuning their structural and optical properties, making them promising candidate for applications in photocatalysis, antibacterial activity, and other advanced functional materials, while also offering a sustainable and eco-friendly approach to nanomaterial synthesis.

Acknowledgements

Author Ms. Shubhangi R. Pawar would like to acknowledge the Mahatma Joyita Phule Research Fellowship (MJPRF-2022), Government of Maharashtra, India. for providing financial assistance. The author also acknowledges the Department of Zoology, Yashavantrao Chavan Institute of Science, Satara, Maharashtra, India, for providing laboratory facilities and the Department of Zoology, Shivaji University, Kolhapur, for continuous support and encouragement throughout the work.

Funding

This work was supported by [Mahatma Jyotiba Phule Research Fellowship (MJPRF-2022), Government of Maharashtra, India]. Grant numbers [Fellowship2022_30]. Author Ms. Shubhangi R. Pawar has received research support from the Mahatma Jyotiba Phule Research Fellowship (MJPRF-2022), Government of Maharashtra, India.

Ethics declarations: Not applicable.

Conflict of Interest

The authors declare that they have no known competing financial interests or personal relationships that could have appeared to influence the work reported in this paper

REFERENCES

1. Parveen, K.; Banse, V.; Ledwani, L. Green Synthesis of Nanoparticles: Their Advantages and Disadvantages. 2016. https://doi.org/10.1063/1.4945168.
2. Balamurughan, M.G. & Sunderasan, Mohanraj & Kodhaiyolii, S. & Pugalenthi, V.. (2014). *Ocimum sanctum* leaf extract mediated green synthesis of iron oxide nanoparticles: Spectroscopic and microscopic studies. Journal of Chemical and Pharmaceutical Sciences. 2014. 201-204.
3. Abdullah, A.; Jiménez-Rosado, M.; Guerrero, A.; Romero, A. Effect of Calcination Temperature and Time on the Synthesis of Iron Oxide Nanoparticles: Green vs. Chemical Method. *Materials* **2023**, *16* (5), 1798–1798. https://doi.org/10.3390/ma16051798.
4. Hassan, Y. M.; Zaid, H. M.; Guan, B. H.; Hamza, M. F.; Adam, A. A. Effect of Annealing Temperature on the Crystal and Morphological Sizes of Fe_2O_3/SiO_2 Nanocomposites. *IOP Conference Series: Materials Science and Engineering* **2021**, *1092* (1), 012039. https://doi.org/10.1088/1757-899x/1092/1/012039.
5. Alagu, T. SYNTHESIS and IMPREGNATION of Fe2O3 NANOPARTICLES on CELLULOSE PAPER and SODIUM ALGINATE FILMS for the PRESERVATION of FRUIT and VEGETABLES. *Journal of Microbiology,*

Biotechnology and Food Sciences **2020**, *9* (6), 1166–1169. https://doi.org/10.15414/jmbfs.2020.9.6.1166-1169.

6. Thakur, M.; Poojary, S.; Swain, N. Green Synthesis of Iron Oxide Nanoparticles and Its Biomedical Applications. *Nanotechnology in the Life Sciences* **2021**, 83–109. https://doi.org/10.1007/978-3-030-64410-9_5.
7. Chakraborty, A. R.; Tuz, F.; Alam, K.; Yousuf, S. B.; Hossain, K. S. Influence of Annealing Temperature on Fe_2O_3 Nanoparticles: Synthesis Optimization and Structural, Optical, Morphological, and Magnetic Properties Characterization for Advanced Technological Applications. *Heliyon* **2024**, *10* (21), e40000–e40000. https://doi.org/10.1016/j.heliyon.2024.e40000
8. Federica Crippa; Rodriguez-Lorenzo, L.; Hua, X.; Goris, B.; Bals, S.; Garitaonandia, J. S.; Balog, S.; Burnand, D.; Hirt, A. M.; Laetitia Haeni; Lattuada, M.; Rothen-Rutishauser, B.; Alke Petri-Fink. Phase Transformation of Superparamagnetic Iron Oxide Nanoparticles via Thermal Annealing: Implications for Hyperthermia Applications. *ACS Applied Nano Materials* **2019**, *2* (7), 4462–4470. https://doi.org/10.1021/acsanm.9b00823.
9. Khan, M. A.; Ahmed, M.; Abu-Hussien, S. H.; Zahid, M. U.; Alharbi, B. F. Green Synthesis of Iron Oxide Nanoparticles (Fe2O3-NPs) from Citrus Limetta Agrowaste for Biological and Photocatalytic Applications. *Scientific Reports* **2025**, *15* (1). https://doi.org/10.1038/s41598-025-17750-3.
10. Singh, A. K. A Review on Plant Extract-Based Route for Synthesis of Cobalt Nanoparticles: Photocatalytic, Electrochemical Sensing and Antibacterial Applications. *Current Research in Green and Sustainable Chemistry* **2022**, *5*, 100270. https://doi.org/10.1016/j.crgsc.2022.100270.
11. N, G.; Michael, R. Green Synthesis of Iron Oxide Nanoparticles Using the Leaf Extract of Phyllanthus Niruri. *Nanoscale Reports* **2020**, *3* (3). https://doi.org/10.26524/nr.3.18.
12. Buarki, F.; AbuHassan, H.; Al Hannan, F.; Henari, F. Z. Green Synthesis of Iron Oxide Nanoparticles Using Hibiscus Rosa Sinensis Flowers and Their Antibacterial Activity. *Journal of Nanotechnology* **2022**, *2022*, 1–6. https://doi.org/10.1155/2022/5474645.
13. Ibtihal Mimouni; Asmae Bouziani; Yassine Naciri; Mourad Boujnah; Alaoui, M.; Mohammed El Azzouzi. Effect of Heat Treatment on the Photocatalytic Activity of α-Fe2O3 Nanoparticles: Towards Diclofenac Elimination. *Environmental Science and Pollution Research* **2021**, *29* (5), 7984–7996. https://doi.org/10.1007/s11356-021-16146-w.
14. Xu, X. N.; Wolfus, Y.; Shaulov, A.; Yeshurun, Y.; Felner, I.; Nowik, I.; Koltypin, Yu.; Gedanken, A. Annealing Study of Fe2O3 Nanoparticles: Magnetic Size Effects and Phase Transformations. *Journal of Applied Physics* **2002**, *91* (7), 4611–4616. https://doi.org/10.1063/1.1457544.
15. Ndou, Nzumbululo & Rakgotho, Tessia & Nkuna, Mulisa & Ibrahima Zan, Doumbia & Mulaudzi-Masuku, Takalani & Ngece-Ajayi, Rachel. (2023). Green Synthesis of Iron Oxide (Hematite) Nanoparticles and Their Influence on Sorghum bicolor Growth under Drought Stress. Plants. 12. 1425. https://doi.org/10.3390/plants12071425
16. Aida, M.s & Alonizan, Norah & Zarrad, Boubaker & Hjiri, M.. (2023). Green synthesis of iron oxide nanoparticles using Hibiscus plant extract. Journal of Taibah University for Science. 17.

https://doi.org/10.1080/16583655.2023.2221827

17. Jesus, Juliana & Regadas, Joana & Costa, Bárbara & Carvalho, João & Pádua, Ana & Henriques, Célia & Soares, Paula & Gavinho, Sílvia & Valente, Manuel & Graça, Manuel & Teixeira, S. (2024). Green Sol–Gel Synthesis of Iron Oxide Nanoparticles for Magnetic Hyperthermia Applications. Pharmaceutics. 16. 1578. https://doi.org/10.3390/pharmaceutics16121578
18. Edvinsson, T. Optical Quantum Confinement and Photocatalytic Properties in Two-, One- and Zero-Dimensional Nanostructures. *Royal Society Open Science* **2018**, *5* (9), 180387. https://doi.org/10.1098/rsos.180387.

HOW TO CITE: Shubhangi Pawar, Nilesh Pandit, Rajan More, Effect of Annealing Temperature on the Structural and Physicochemical Properties of Green-Synthesized Iron Oxide Nanoparticles from Ocimum sanctum, Int. J. of Pharm. Sci., 2026, Vol 4, Issue 5, 6827-6844, https://doi.org/10.5281/zenodo.20392833